Development in the short- and medium-range structure in amorphous $Ca_{10}Mg_{90-x}Ga_x$ $(0 \leqslant x \leqslant 40)$ alloys

1998 J. Phys.: Condens. Matter 10 10179

(http://iopscience.iop.org/0953-8984/10/45/006)

J. Phys.: Condens. Matter **10** (1998) 10179–10192. Printed in the UK PII: S0953-8984(98)95440-6

Development in the short- and medium-range structure in amorphous $Ca_{10}Mg_{90-x}Ga_x$ ($0 \leqslant x \leqslant 40$) alloys

Nobuhiko Takeichi, Toshiharu Fukunaga† and Uichiro Mizutani

Department of Crystalline Materials Science, Nagoya University, Furo-cho, Chikusa-ku, Nagoya 464-8603, Japan

Received 29 June 1998, in final form 25 August 1998

Abstract. Detailed atomic structure analysis has been made for a series of the amorphous $Ca_{10}Mg_{90-x}Ga_x$ ($0 \leqslant x \leqslant 40$) alloys by utilizing a combination of both neutron and x-ray diffraction techniques. The structure factors $S_{Mg}(Q)$ and $S_{Ga}(Q)$ associated with the atomic environment around Mg and Ga atoms can be deduced from the two sets of the total $S(Q)$ obtained from neutron and x-ray diffractions. A prepeak is found to grow at $Q \approx 1.65$ Å in $S_{Ga}(Q)$ but not in $S_{Mg}(Q)$, when Ga concentration exceeds 15 at.%. Its appearance can be interpreted as the formation of the medium-range structure characteristic of the (110) lattice planes composed of all Ga atoms in the Mg_2Ga crystalline compound. The coordination number and atomic distance of the Mg–Mg, Mg–Ga and Mg–Ca atomic pairs can be deduced by decomposing the first main peak of the RDF(r) obtained by Fourier transforming $S_{Mg}(Q)$ for all amorphous alloys studied. We showed that the Mg_2Ga-type short-range structure develops and the Mg–Ga atomic distance is shortened to the level of 2.9 Å for samples with $x \geqslant 20$. This is attributed to the formation of the bonding state between Mg and Ga atoms. It is also found that the Mg_2Ca-type short-range structure, where each Ca atom is fully surrounded by Mg atoms, persists up to $x = 10$. However, the Ga–Ca atomic pair gradually grows with increasing Ga concentration above $x = 15$.

1. Introduction

Fukunaga *et al* [1] deduced from a combination of neutron and x-ray diffraction studies that the Al–Cu and Al–Y bonding states grow with increasing Al concentration in the amorphous $Al_x(Cu_{0.4}Y_{0.6})_{100-x}$ ($0 \leqslant x \leqslant 85$) alloys and attributed the observed rapid increase in resistivity and the reversal of a sign of the Hall coefficient from a negative to positive one to the growth of the short-range order in the ternary amorphous alloys. Indeed, the formation of the Al–Y and Al–Cu bonding states near the Fermi level has been experimentally confirmed by x-ray photoemission spectroscopy and soft x-ray Al Kβ and Cu L$\alpha_{1,2}$ emission spectroscopy [1]. Moreover, Takeichi *et al* [2] successfully calculated the atomic structure of the amorphous $Al_x(Cu_{0.4}Y_{0.6})_{100-x}$ ($x = 30$ and 80) alloys in molecular dynamics simulations by adjusting the parameters involved so as to reconcile the resulting radial distribution function (RDF(r)) with the measured one as closely as possible. By using the atomic structure thus constructed, they further calculated the valence band structure in the linear muffin-tin orbital (LMTO) recursion method and could reproduce well the bonding states near the Fermi level consistent with the observed photoemission spectra.

† Present address: Research Reactor Institute, Kyoto University, Kumatori-Cho, Sennan-gun, Osaka 590-0494, Japan.

0953-8984/98/4510179+14$19.50

A series of these experimental and theoretical works could clearly demonstrate that the short-range atomic structure affects significantly the valence band structure near the Fermi level and is responsible for the manifestation of unique electron transport properties. In the following paper, we show that the electrical resistivity at 300 K for the amorphous $Ca_{10}Mg_{90-x}Ga_x$ alloys is only 53 $\mu\Omega$ cm for $x = 0$ but increases to 215 $\mu\Omega$ cm when the Ga concentration is increased to 30. We consider a rapid increase in resistivity to originate from the formation of bonding states near the Fermi level as a result of the development of short-range structures. In the present work, we determined the local atomic structure for amorphous $Ca_{10}Mg_{90-x}Ga_x$ alloys ($0 \leqslant x \leqslant 40$) as a function of Ga concentration x by using both x-ray and neutron diffraction techniques in the same way as we have done for the amorphous $Al_x(Cu_{0.4}Y_{0.6})_{100-x}$ alloys [1].

2. Experiment

A total of six $Ca_{10}Mg_{90-x}Ga_x$ ($x = 0$, 10, 15, 20, 30 and 40) alloy ingots was prepared by induction melting appropriate amounts of 99.5% Ca, 99.9% Mg and 99.999% Ga in vacuum. A single-roll melt-spinning apparatus was operated in the reduced Ar gas atmosphere to produce a rapidly quenched ribbon sample. The Cu roll with 20 cm in diameter was spun with a rotating speed of 5000 rpm. A resulting ribbon sample is about 1 mm in width, 30 μm in thickness and a few cm in length. The x-ray diffraction studies with Cu Kα radiation revealed that all samples in the composition range $0 \leqslant x \leqslant 40$ are in an amorphous single phase but the sample with $x = 45$ is partially crystallized. A deviation from the nominal composition in all amorphous samples is found to be within $\pm 1\%$, as revealed by the energy dispersive x-ray analyser (Seiko Instruments, SII).

The thermal stability of each amorphous sample was studied with the differential scanning calorimeter (DSC) (Rigaku-8121BH) at a heating rate of 15 K min^{-1}. The crystallization temperature is determined by reading off the temperature corresponding to an initial rise of the exothermic peak in the DSC spectrum. The mass density, which is needed in the derivation of RDF(r) from the structure factor $S(Q)$, was measured by using the Archimedes method with toluene as a working fluid. All amorphous samples were slowly oxidized, if left in air. Hence, each sample was sealed in a Pyrex glass tube under vacuum and kept in a refrigerator until the measurement was carried out.

The structure factor $S(Q)$ for the present amorphous alloy was determined by measuring both x-ray and neutron diffraction spectra. Amorphous ribbons were collected so as to total approximately 1–2 g in weight for the neutron diffraction experiment. Mo Kα radiation (50 kV and 30 mA) monochromatized with the (002) plane of graphite was employed in a step-scanning mode in the x-ray diffraction studies. The neutron diffraction measurement was carried out by using the high-intensity total scattering spectrometer (HIT-II) installed at a spallation pulsed-neutron source generated from a 500 MeV proton booster synchrotron at the High Energy Accelerator Research Organization (KEK, Japan).

3. Results and discussion

3.1. Thermal properties

Figure 1 shows a set of the DSC spectra obtained by heating the amorphous sample up to 550 K. A sharp exothermic peak was observed for all samples studied, indicating that

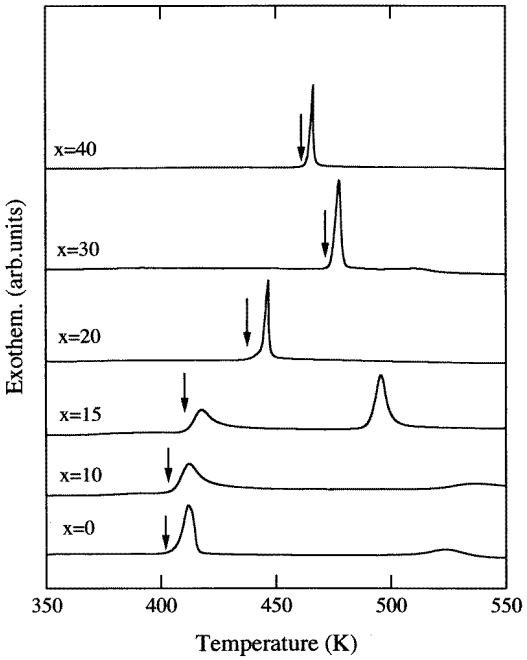

Figure 1. DSC spectra for a series of the amorphous $Ca_{10}Mg_{90-x}Ga_x$ $(0 \leqslant x \leqslant 40)$ alloys. The crystallization temperature T_x is determined from the onset of the exothermic peak as marked by an arrow.

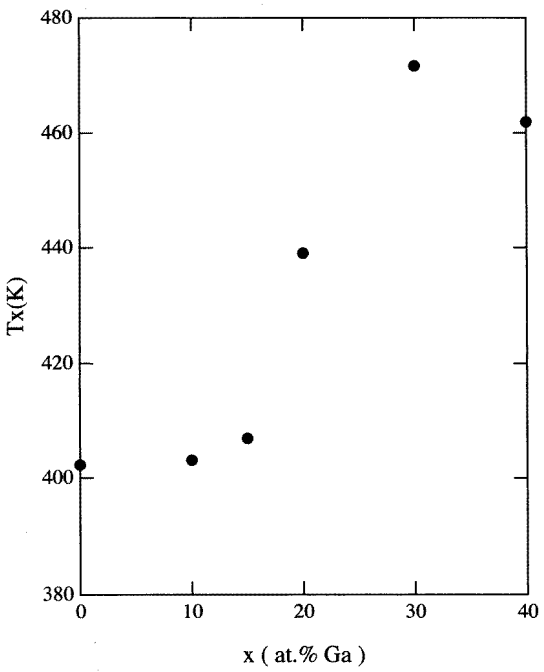

Figure 2. The Ga concentration dependence of crystallization temperature T_x in the amorphous $Ca_{10}Mg_{90-x}Ga_x$ $(0 \leqslant x \leqslant 40)$ alloys.

the melt-spun sample was indeed in an amorphous phase. The crystallization temperature T_x is defined as the temperature at which an exothermic peak initiates, as marked by an arrow in figure 1. Numerical values are listed in table 1, together with the mass density. The Ga concentration dependence of T_x is shown in figure 2. It increases rapidly when the Ga concentration x exceeds 20 at.% but tends to level off above $x = 30$. An increase in T_x with increasing Ga content above $x = 20$ is indicative of the formation of the strong bonding states between already existing Mg or Ca atoms and the newly added Ga atoms. It may be noted that some samples exhibited two successive exothermic peaks in the DSC spectra. However, we were unable to identify whether a new crystalline phase is formed when the sample is heated above the second exothermic peak.

Table 1. The mass density and the crystallization temperature of amorphous $Ca_{10}Mg_{90-x}Ga_x$ ($0 \leqslant x \leqslant 40$) alloys.

x	d (g cm^{-3})	T_x (K)
0	1.71	402
10	2.09	403
15	2.34	407
20	2.56	439
30	3.02	472
40	3.47	462

The crystallized phases obtained by heating the amorphous sample up to 673 K were analysed by means of the x-ray diffractometer with Cu Kα radiation. The amorphous $Ca_{10}Mg_{90}$ binary alloy is found to decompose into pure Mg and the $MgZn_2$-type C-12 Laves Mg_2Ca compound. The x-ray diffraction peaks associated with the Mg_2Ca compound have gradually decreased with increasing Ga concentration and disappeared completely when x reaches 20. Instead, the formation of the $LiSb_2$-type Mg_2Ga compound was identified to grow for the crystallized samples with $x \geqslant 30$. Unfortunately, however, there are still a number of diffraction lines which cannot be identified in terms of existing compounds.

Figure 3(a) shows the Mg and Ca concentration profiles in the crystallized $Ca_{10}Mg_{90}$ alloy taken with the electron-probe microanalyser in the line scanning mode (EPMA-1400, Shimazu). It is clear that the peaks in the Ca spectrum are always found at the positions where Mg is scarce and are roughly separated at every few μm apart from each other. Keeping in mind an extremely high Mg concentration of 90 at.% and the decomposition into Mg and Mg_2Ca compound, we believe that the Mg_2Ca compound of the order of a few μm in size is segregated in the essentially pure Mg matrix. Unfortunately, no electron microscopy measurement was attempted in this experiment to estimate the size of the precipitated Mg_2Ca compound.

Similar data were taken for the crystallized ternary alloys. Here the Ga line profile was also measured. The resulting profiles for all samples happen to be similar to each other within the resolution of about 1 μm, irrespective of the Ga concentration x. The data for $x = 30$ are shown in figure 3(b) as representative. It can be seen that the Ca spectrum exhibits peaks with different intensities every few μm apart and that the Ca peak always appears at the position where intensities of both Mg and Ga profiles are lower than their averages. This is consistent with the formation of the Mg_2Ga compound, as identified by the x-ray diffraction. It may be also suggestive that Ca atoms tend to be excluded from the Mg_2Ga compound.

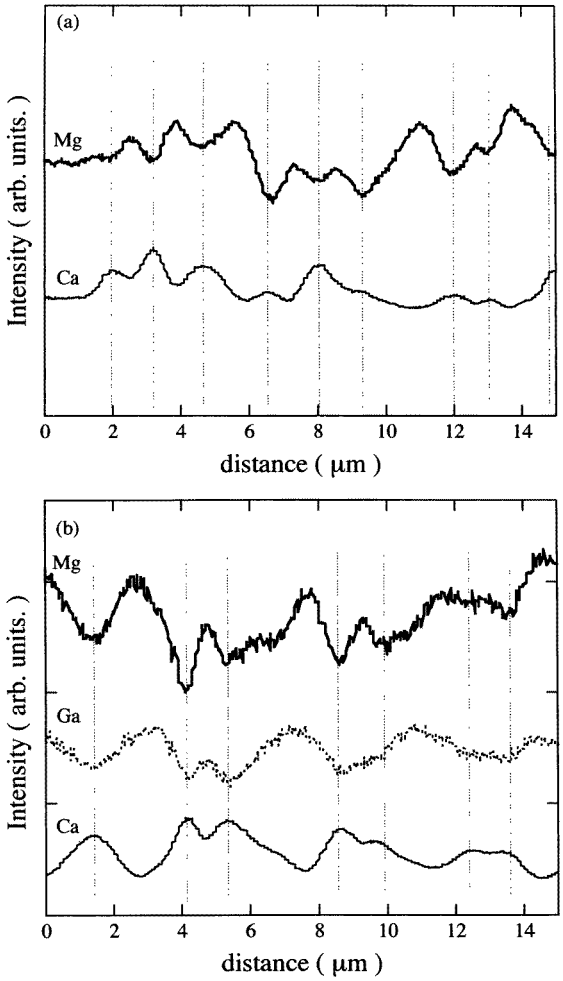

Figure 3. Line scanned concentration profiles for crystallized (a) $Ca_{10}Mg_{90}$ and (b) $Ca_{10}Mg_{60}Ga_{30}$ alloys. Mg: thick line, Ca: thin line and Ga: dotted line.

3.2. Determination of structure factors and medium-range order

Figures 4 and 5 show the structure factor $S(Q)$ derived from x-ray and neutron diffraction experiments for a series of amorphous $Ca_{10}Mg_{90-x}Ga_x$ alloys. It is clearly seen that a prepeak grows at about $Q \approx 1.65$ Å^{-1} in the x-ray structure factor for samples with $x \geqslant 15$. In contrast, the prepeak is absent in the $x = 0$ and 10 samples. Such a prepeak has been attributed to the presence of the medium-range structure in amorphous SiO_2 [3] and amorphous Se [4]. The existence of the prepeak has been reported also in several metallic glasses like Ni–Ti [5–7] and Ni–Zr [8]. Hence, the appearance of the prepeak is likely attributed to the development of the medium-range order in the present samples with $x \geqslant 15$. In all cases mentioned above, the prepeak is believed to originate from the presence of some correlations between the structural units like tetrahedral units typically observed in many amorphous alloys [9]. In the present work, we use the term 'medium-range' structure only in connection with the observed prepeak.

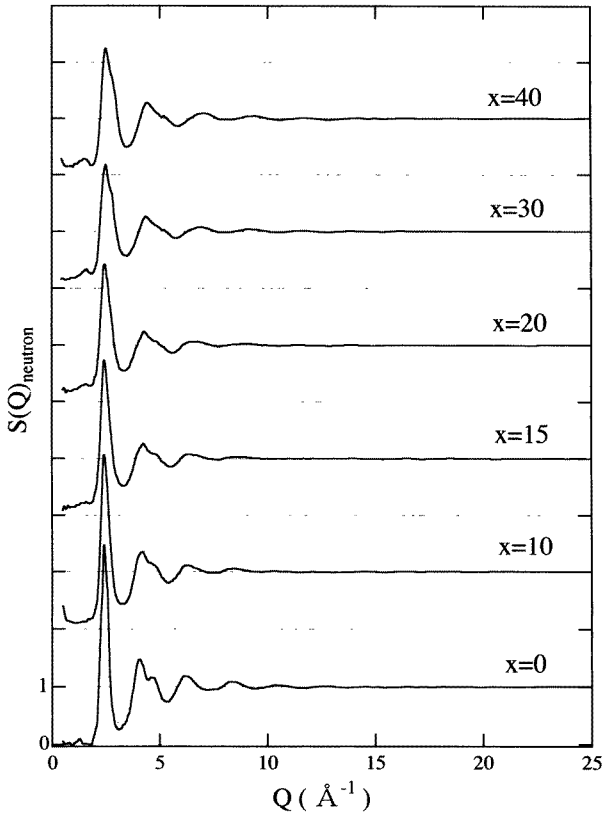

Figure 4. The neutron structure factor $S(Q)_{neutron}$ for a series of the amorphous $Ca_{10}Mg_{90-x}Ga_x$ $(0 \leqslant x \leqslant 40)$ alloys.

In order to gain further insight into the atomic structure for the amorphous $Ca_{10}Mg_{90-x}Ga_x$ alloys, we have decomposed the x-ray and neutron $S(Q)$ for the present ternary amorphous alloys into the partial structure factors in the Faber–Ziman representation. The total $S(Q)$ can be expressed as a weighted sum of six partial structure factors in the following form:

$$S(Q) = \frac{1}{\langle b\rangle^2}[c_{Mg}^2 b_{Mg}^2 S_{MgMg}(Q) + c_{Ca}^2 b_{Ca}^2 S_{CaCa}(Q) + c_{Ga}^2 b_{Ga}^2 S_{GaGa}(Q) + 2c_{Mg}c_{Ca}b_{Mg}b_{Ca}S_{MgCa}(Q) + 2c_{Mg}c_{Ga}b_{Mg}b_{Ga}S_{MgGa}(Q) + 2c_{Ca}c_{Ga}b_{Ca}b_{Ga}S_{CaGa}(Q)] \quad (1)$$

with $\langle b\rangle$ defined as

$$\langle b\rangle = c_{Mg}b_{Mg} + c_{Ca}b_{Ca} + c_{Ga}b_{Ga} \quad (2)$$

where c_i and b_i are the concentration and coherent scattering amplitude of the type i atom, respectively.

To proceed further, we have made full use of the fact that the ratio of the neutron scattering amplitude to the x-ray scattering factor happens to be equal to 4.25 for both Ca and Ga atoms. This implies that the weighting factors of the Ca–Ca, Ca–Ga and Ga–Ga pair correlations in the x-ray structure factor $S(Q)_{x\text{-}ray}$ can be simultaneously equalized to

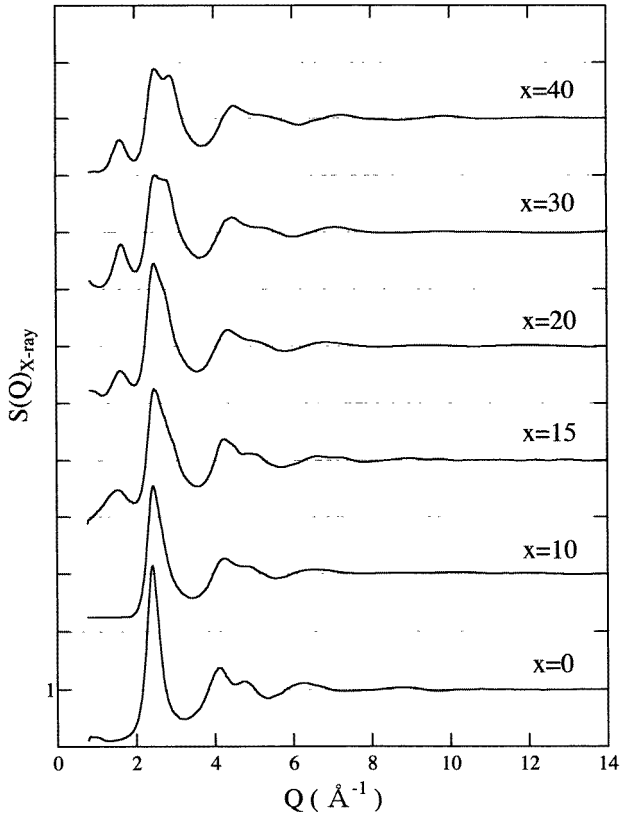

Figure 5. The x-ray structure factor $S(Q)_{x\text{-}ray}$ taken with Mo Kα radiation for a series of amorphous $Ca_{10}Mg_{90-x}Ga_x$ ($0 \leqslant x \leqslant 40$) alloys.

those in the neutron structure factor $S(Q)_{neutron}$ by multiplying an appropriate factor and that the Ca–Ca, Ca–Ga and Ga–Ga pair correlations can be eliminated at once from the six pair correlations in the $S(Q)$. For example, $S(Q)_{x\text{-}ray}$ and $S(Q)_{neutron}$ for the amorphous $Ca_{10}Mg_{60}Ga_{30}$ alloy are expressed as follows:

$$S(Q)_{neutron} = 0.300\,675S_{MgMg}(Q) + 0.006\,386S_{CaCa}(Q) + 0.138\,19S_{GaGa}(Q) + 0.087\,639S_{MgCa}(Q) + 0.407\,0688S_{MgGa}(Q) + 0.059\,415S_{CaGa}(Q) \qquad (3)$$

and

$$S(Q)_{x\text{-}ray} = 0.151\,468S_{MgMg}(Q) + 0.011\,687S_{CaCa}(Q) + 0.252\,710S_{GaGa}(Q) + 0.084\,149S_{MgCa}(Q) + 0.391\,293S_{MgGa}(Q) + 0.108\,692S_{CaGa}(Q). \qquad (4)$$

By multiplying a factor of 1.829 by both sides of equation (3) with its subsequent subtraction from equation (4), we can simultaneously eliminate the partial structure factors $S_{CaCa}(Q)$, $S_{CaGa}(Q)$ and $S_{GaGa}(Q)$. The resulting structure factor $S_{Mg}(Q)$ is explicitly written as

$$S_{Mg}(Q) \equiv \frac{1}{0.829}[1.829S_{neutron}(Q) - S_{x\text{-}ray}(Q)] = 0.480\,673S_{MgMg}(Q) + 0.427\,476S_{MgGa}(Q) + 0.091\,8508S_{MgCa}(Q). \qquad (5)$$

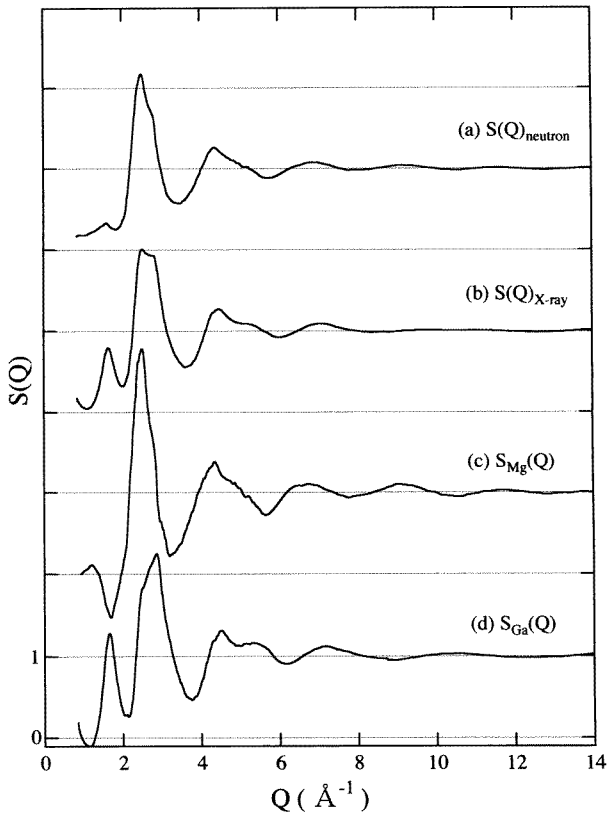

Figure 6. Structure factors for the amorphous $Ca_{10}Mg_{60}Ga_{30}$ alloy. (a) $S(Q)_{neutron}$, (b) $S(Q)_{x\text{-}ray}$, (c) $S_{Mg}(Q)$ and (d) $S_{Ga}(Q)$.

It is clear from equation (5) that $S_{Mg}(Q)$ is composed of only Mg–Mg, Mg–Ga and Mg–Ca correlations and reflects the atomic environment around an Mg atom in the present ternary amorphous alloys.

As a next step, we may eliminate $S_{MgMg}(Q)$ from equations (3) and (4). The resulting structure factor is denoted as $S_0(Q)$ and is explicitly written for the $x = 30$ sample in the form of

$$S_0(Q) = 0.017\,069 S_{CaCa}(Q) + 0.368\,959 S_{GaGa}(Q) + 0.084\,149 S_{MgCa}(Q) + 0.374\,649 S_{MgGa}(Q) + 0.158\,717 S_{CaGa}(Q) \quad (6)$$

where the weighting factors of the Ca–Ca and Mg–Ca correlations are so small relative to those of the Ga–Ga, Mg–Ga and Ca–Ga correlations that they are well neglected. Thus, equation (6) for the sample with $x = 30$ is approximated as

$$S_0(Q) = 0.368\,959 S_{GaGa}(Q) + 0.374\,649 S_{MgGa}(Q) + 0.158\,717 S_{CaGa}(Q). \quad (7)$$

Equation (7) represents well the atomic environment around a Ga atom. This holds true for all Ga-rich amorphous alloys. Thus, the structure factor $S_0(Q)$ for the amorphous alloys with $x \geqslant 30$ is hereafter denoted as $S_{Ga}(Q)$.

Figure 6 shows various structure factors, which include (a) $S(Q)_{x\text{-}ray}$, (b) $S(Q)_{neutron}$, (c) $S_{Mg}(Q)$ and (d) $S_{Ga}(Q)$ for the amorphous $Ca_{10}Mg_{60}Ga_{30}$ alloy. A prepeak located at

$Q \approx 1.65$ Å^{-1} is visible only in $S(Q)_{x\text{-}ray}$ and $S_{Ga}(Q)$, indicating that the prepeak *does* originate from the atomic environment around the Ga atom. More specifically, it must be due to the Ga–Ga correlation, since its absence in $S_{Mg}(Q)$ indicates the prepeak to have nothing to do with the Mg–Ga correlation. It is of great interest to note that the prepeak is located in the vicinity of the (110) diffraction peak of the Mg_2Ga compound. The Mg_2Ga compound is known to crystallize into the hexagonal structure with 12 Mg atoms and six Ga atoms in the unit cell [10]. All Ga atoms lie on the (110) plane with their interplanar spacing of 3.95 Å. This is converted to the wave number of 1.61 Å^{-1} through the relation $Q = 4\pi \sin(\theta/2)/\lambda$, where λ is the wavelength of the incident x-ray beam and θ is the scattering angle. We see that the position of the observed prepeak agrees well with the wave number of 1.61 Å^{-1} corresponding to the (110) interplanar spacing of the Mg_2Ga compound. Thus, we believe that the medium-range structure characteristic of the layered Ga(110) planes in the Mg_2Ga compound remains in the present amorphous $Ca_{10}Mg_{90-x}Ga_x$ alloys with $x \geqslant 15$.

3.3. Radial distribution function and short-range atomic structures

Figure 7 shows the radial distribution function $\mathrm{RDF}_{Mg}(r)$ obtained by Fourier transforming $S_{Mg}(Q)$ for the present amorphous alloys. Prior to the interpretation of the $\mathrm{RDF}_{Mg}(r)$ data,

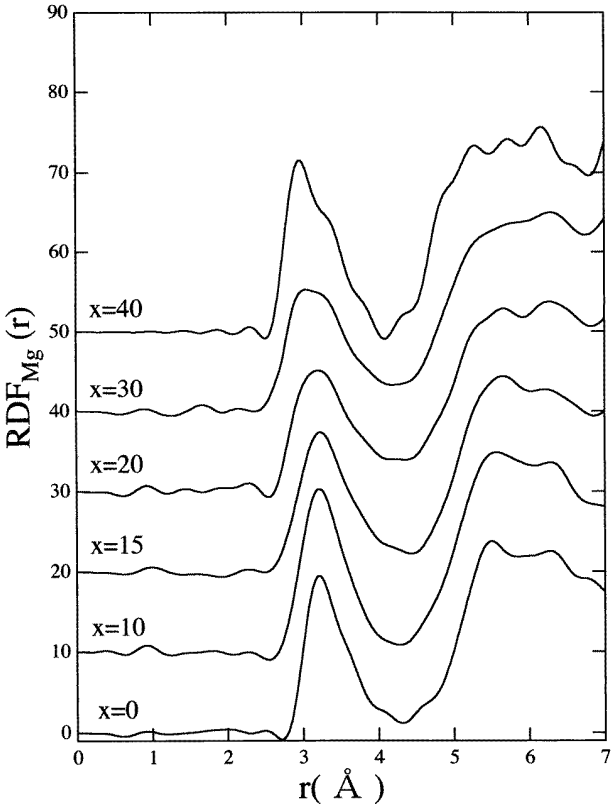

Figure 7. The radial distribution function (RDF(r)) around the Mg atom obtained by the Fourier transformation of $S_{Mg}(Q)$ for a series of the amorphous $Ca_{10}Mg_{90-x}Ga_x$ $(0 \leqslant x \leqslant 40)$ alloys.

it is worthwhile mentioning that interatomic distances of atomic pairs Mg–Ca, Mg–Mg and Mg–Ga are expected to be 3.57, 3.2 and 2.94 Å, respectively, if the hard sphere model with the Goldschmidt radii of $r_{Ca} = 1.97$, $r_{Mg} = 1.60$ and $r_{Ga} = 1.34$ Å is applied. In addition, it is worthwhile noting that the term 'short-range atomic structure' is used in the present work to describe the atomic structure deduced from the main peak of the partial RDF(r). Being guided by the hard sphere model, we can naturally interpret the first peak centred at 3.2 Å of the amorphous $Ca_{10}Mg_{90}$ alloy as arising from the Mg–Mg atomic pair. A small shoulder at about 3.6 Å on the right-hand side of the first peak is definitely attributed to the Mg–Ca correlation. The shoulder at 3.6 Å remains visible in spite of an increase in Ga concentration to $x = 40$, indicating that the Mg–Ca correlation apparently persists throughout the stable amorphous composition range. The shoulder also grows at about 2.9 Å for the samples with $x \geqslant 20$. It is even slightly visible for the $x = 15$ sample. This is safely ascribed to the growth of the Mg–Ga atomic pair. Indeed, the number of the Mg–Ga atomic pairs gradually increases with increasing Ga concentration and eventually grows into the first main peak when x reaches 40. It is interesting to note that the Mg–Ga correlation grows in harmony with the growth of the Ga–Ga prepeak mentioned above.

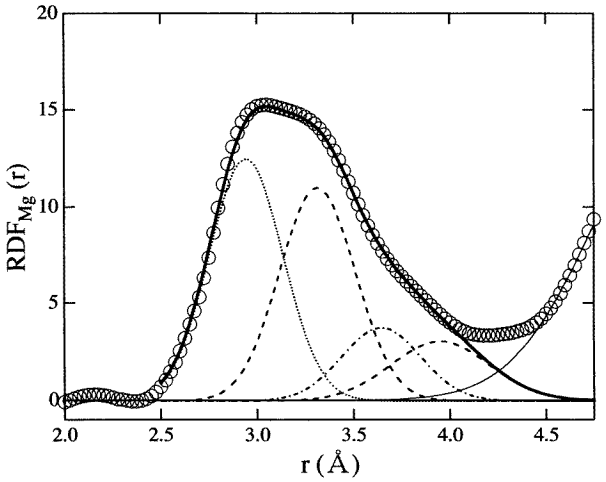

Figure 8. Decomposition of the first RDF(r) peak into four partials due to Mg–Ga, Mg–Mg (1), Mg–Ca and Mg–Mg (2) pairs in the amorphous alloy with $x = 30$. The second RDF(r) peak centred at about 6 Å has a tail to about 4 Å. This contribution is approximated as a thin solid curve and is subtracted before decomposing the first peak into the four partials. Open circles: data points, dotted line: Mg–Ga, dashed line: Mg–Mg (1) and (2), dashed–dotted line: Mg–Ca and thick solid line: total fitting curve.

The first peak in RDF$_{Mg}(r)$ for a series of the present amorphous alloys can be decomposed into the partial RDF(r) due to Mg–Ga, Mg–Mg and Mg–Ca pairs by approximating each with the Gaussian distribution function. This allows us to deduce the nearest neighbour atomic distance and its coordination number for these atomic pairs. A typical example is shown in figure 8 for the $x = 30$ sample. The first peak can be successfully decomposed into four partials Mg–Ga, Mg–Mg (1), Mg–Ca and Mg–Mg (2), where Mg–Mg (1) and Mg–Mg (2) correspond to Mg–Mg pairs at the nearest and second nearest neighbours, respectively. Here we attributed the fourth partial RDF(r) centred at 3.9 Å to Mg–Mg atomic pairs in the second nearest neighbour distance, as will be discussed below.

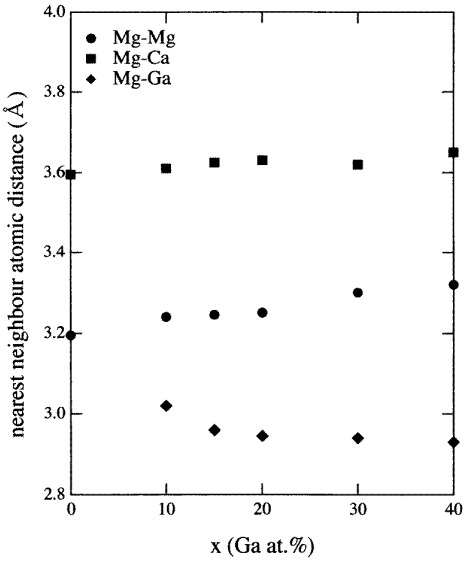

Figure 9. The Ga concentration dependence of the nearest neighbour atomic distance for the Mg–Mg, Mg–Ca and Mg–Ga atomic pairs for a series of the amorphous $Ca_{10}Mg_{90-x}Ga_x$ ($0 \leqslant x \leqslant 40$) alloys.

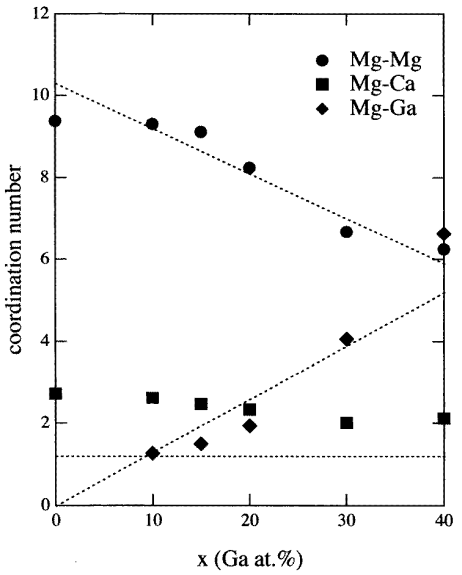

Figure 10. The Ga concentration dependence of the coordination number for the Mg–Mg, Mg–Ca and Mg–Ga atomic pairs for a series of the amorphous $Ca_{10}Mg_{90-x}Ga_x$ ($0 \leqslant x \leqslant 40$) alloys. Three straight lines represent the coordination number expected from the random distribution model.

The resulting nearest neighbour atomic distance is plotted as a function of the Ga concentration in figure 9. As noted above, the Mg–Mg nearest neighbour distance gradually increases with increasing Ga concentration, while the Mg–Ca distance remains almost unchanged. More important to be noted is that the Mg–Ga distance initially decreases sharply with increasing Ga concentration but levels off at the value of 2.93 Å for samples with $x \geqslant 20$. There are several different atomic spacings for the Mg–Ga and Mg–Mg pairs in the Mg_2Ga compound. The atomic spacing of the Mg–Ga pair is centred at about 2.9 and 4.2 Å in good agreement with that found in the present samples with $x \geqslant 20$. On the other hand, the atomic spacing of the Mg–Mg pairs is distributed in the neighbourhood of 3.2 and 3.9 Å in the Mg_2Ga compound, being again consistent with the present data shown in figure 8. All these results indicate that the Mg_2Ga-like short-range structure grows for samples with $x \geqslant 20$.

Figure 10 shows the Ga concentration dependence of the coordination number for the three atomic pairs. Dashed lines in figure 10 represent the Ga concentration dependence of the coordination number calculated by assuming that all three constituent atoms are randomly distributed in the amorphous matrix. Obviously, the coordination number of the Mg–Mg atomic pair decreases almost linearly in an excellent agreement with the random distribution model. In contrast, the increase in the coordination number of the Mg–Ga atomic pair is far less than that expected from the random distribution model for samples with $x \leqslant 20$ but catches up with the value when x exceeds 30.

Another interesting feature is found in the Mg–Ca atomic pair. According to the random distribution model, the coordination number of the Mg–Ca atomic pair must be independent of Ga concentration and centred at about 1.2–1.3, if the total coordination number is taken to

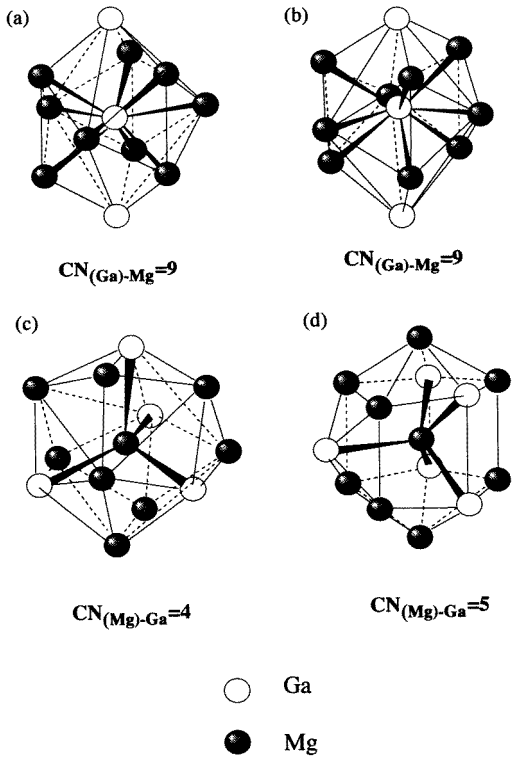

Figure 11. The atomic arrangements in the Mg_2Ga compound. (a) and (b): Mg atoms around Ga atom. (c) and (d): Ga atoms around Mg atom. $CN_{(A)-B}$ indicates the coordination number of B atoms around A atom.

be 12 or 13. Thus, its value of 2.7 for the amorphous $Ca_{10}Mg_{90}$ alloy is unexpectedly higher than that obtained from the random distribution model. The Mg_2Ca compound possesses in total six Ca atoms around the Mg atom at the distances of 3.6–3.65 Å [11]. As shown in figure 9, the atomic distance of the Mg–Ca pair in the amorphous phase is distributed in the vicinity of 3.6 Å. Hence, we consider the Mg_2Ca-type short-range order to be present in the amorphous matrix and to be responsible for an unexpectedly increased coordination number of the Mg–Ca pair.

The $RDF_{Ga}(r)$ around the Ga atom can be obtained by the Fourier transformation of $S_{Ga}(Q)$ given by equation (7) for the Ga-rich samples with $x = 30$ and 40. The decomposition of the resulting $RDF_{Ga}(r)$ into partial contributions must be proceeded with in a way consistent with the results around the Mg atom. The atomic distance of the Mg–Ga atomic pair can be determined from both $RDF(r)$ around Mg and Ga atoms. They must be the same. As long as the random distribution model is appropriate, the coordination number of Ga atoms around Mg must be equal to that of Mg atoms around Ga multiplied by the concentration ratio x_{Mg}/x_{Ga}. As can be seen in figure 10, agreement is reasonable for $x \geqslant 30$. However, this does not mean the validity of the random distribution model for the Mg–Ga correlation. Here it is important to note that the Mg_2Ga compound happens to have an Mg–Ga atomic environment similar to that given by the random distribution model. As shown in figure 11, the coordination numbers of the Mg atoms around Ga and that of

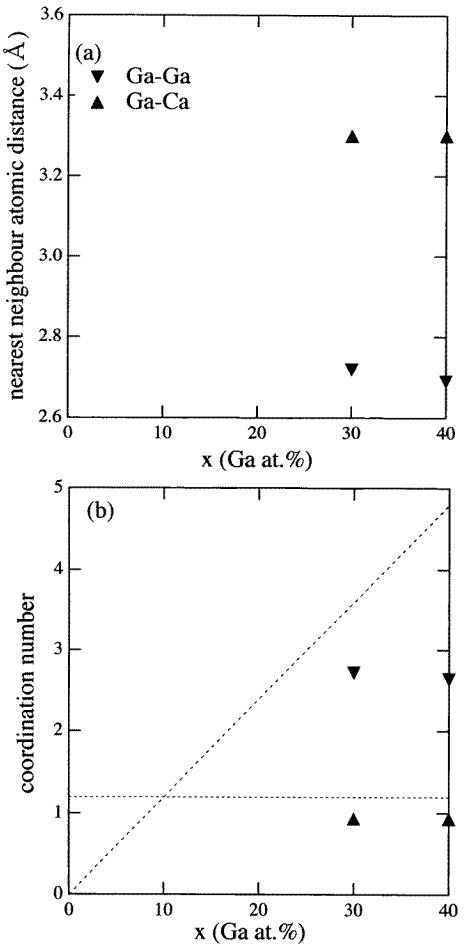

Figure 12. The Ga concentration dependence of (a) the atomic distance and (b) coordination number for the Ga–Ca and Ga–Ga atomic pairs for the amorphous $Ca_{10}Mg_{90-x}Ga_x$ ($x = 30$ and 40) alloys. Dashed lines refer to the coordination number expected from the random distribution model.

the Ga atoms around Mg are 9 and 4.5 in the Mg_2Ga compound, respectively, so that the ratio happens to be equal to $x_{Mg}/x_{Ga} = 2$ for $x = 30$. Thus, by assuming the Mg_2Ga-like short-range order, we have subtracted the Mg–Ga contribution from the $RDF_{Ga}(r)$ and subsequently decomposed the remaining one into the contribution of the Ga–Ga and Ga–Ca atomic pairs for samples for $x \geqslant 30$.

The resulting coordination number and atomic distance of Ga–Ga and Ga–Ca atomic pairs are shown in figure 12 only for samples with $x \geqslant 30$, along with the line expected from the random distribution model. The number of Ca atoms around Ga remains almost unity in agreement with the random distribution model. Instead, the number of Ga atoms around Ga is equal to 2.6 for these two samples and is close to two in the Mg_2Ga compound shown in figure 11(a) and (b). Therefore, we consider that the atomic environment around the Ga atom is well consistent with the formation of the Mg_2Ga-type short-range order in this concentration range.

4. Conclusion

The detailed atomic structure analysis was carried out for a series of the amorphous $Ca_{10}Mg_{90-x}Ga_x$ ($0 \leqslant x \leqslant 40$) alloys by combining both neutron and x-ray diffraction techniques. The structure factors $S_{Mg}(Q)$ and $S_{Ga}(Q)$ associated with the atomic environment around Mg and Ga atoms could be extracted from the two sets of $S(Q)$ obtained from neutron and x-ray diffractions and the corresponding $RDF_{Mg}(r)$ and $RDF_{Ga}(r)$ were calculated.

The following conclusions are deduced from the present studies.

(1) The Mg_2Ga-type medium-range structure, as manifested by the prepeak, clearly appears for all samples with $x \geqslant 20$.

(2) The Mg_2Ga-type short-range structure develops for samples with $x \geqslant 20$. A rapid shortening of the Mg–Ga atomic distance to the level of 2.9 Å may well be taken as the evidence for the formation of the bonding state between Mg and Ga atoms.

(3) The Mg_2Ca-type short-range structure exists in the amorphous $Ca_{10}Mg_{90}$ alloy. The Ca atom is completely surrounded by Mg atoms in the dilute alloys with $x \leqslant 0$.

Acknowledgments

The authors are grateful to postgraduate students Mr S Kajikawa and Mr T Umezawa for their assistance with the sample preparation and structural analysis at the early stage of this work.

References

[1] Fukunaga T, Sugiura H, Takeichi N and Mizutani U 1996 *Phys. Rev.* B **54** 3200
[2] Takeichi N, Sato H and Mizutani U 1997 *J. Phys.: Condens. Matter* **9** 10 145
[3] Misawa M, Price D L and Suzuki K 1983 *J. Non-Cryst. Solids* **57** 447
[4] Misawa M and Suzuki K 1978 *J. Phys. Soc. Japan* **44** 1612
[5] Fukunaga T, Hayashi N, Kai K, Watanabe N and Suzuki K 1983 *Physica* B **120** 352
[6] Fukunaga T, Watanabe N and Suzuki K 1984 *J. Non-Cryst. Solids* **61/62** 343
[7] Fukunaga T, Urai S, Watanabe N and Suzuki K 1988 *J. Phys. F: Met. Phys.* **18** 99
[8] Fukunaga T, Hayashi N, Watanabe N and Suzuki K 1985 *Proc. 5th Int.Conf. on Rapidly Quenched Metals (Würzburg, 1985)* ed S Steeb and H Warlimont, pp 475–8
[9] Suzuki K, Misawa M and Kobayashi Y 1985 *J. Physique Coll.* **8** C8 617
[10] Frank K and Schubert K 1970 *J. Less-Common Met.* **20** 215
[11] Nowotny H 1946 *Z. Metallk.* **37** 31